# Measurement of a Body-Worn Triaxial Sensor for Electromagnetic Field and Exposure Assessment

Christophe roblin[1] and Alain Sibille[1]
[1] LTCI, Télécom ParisTech & CNRS, Paris, France, christophe.roblin@telecom-paristech.fr

***Abstract*— Preliminary measurements of a triaxial sensor placed at different positions of a whole body phantom are presented. Strategies of measurements correction are discussed.**

***Index* EMF exposure, exposimeter, exposure index.**

## I. INTRODUCTION

The Electromagnetic Field (EMF) exposure of the population due to wireless communications (2G, 3G, 4G and WLANs) originates both from Down-Link (DL) emissions incoming from Base Stations (BS) and Access Points (AP), and from Up-Link ones produced by the terminals (cell phones, tablets and lap-tops). Although the main contribution comes generally from the last, the former must be considered as well, as contributions can be competitive for some cases for which both (e.g. in femtocells. Note however that in this case, the EMF levels are particularly low. In any case, DL emissions are continuous whereas UL ones are time limited.

One of the main objectives of the EU FP7 project *Lexnet* is to propose innovative technical solutions to reduce the exposure level of the population, in a global way, without affecting quality of service. The possible improvements are investigated in every parts of the system, both in terms of technology (antennas, sensitivity, wake-up strategy, RRM, power control, etc.) and in terms of architectures and network (NW) management (heterogeneous networks, offloading, densification, etc.). To this end, a new *Exposure Index* (*EI*) merging both UL and DL emissions is defined, noting notably that, up to now, the exposure sources have been considered separately with different "metrics" (the SAR for the UL one and the field level for the DL one). The *EI* aggregates all sources of exposure due to wireless networks (excluding broadcasting, power lines and all other sources) operating in a given area: it takes into account the environment (type of area –urban to rural– and location –indoor, outdoor), the population present in the considered area (apportioned according to several user profiles), the time of day (traffic loading), the NW RATs (2G, 3G, etc.) and layers (macro to femto cells), and terminals usages (voice, data modes, user posture). The *EI* is inherently an average quantity assessed statistically. The Near Field (NF) contribution (UL) is estimated thanks to SAR simulations for various models of sources (terminals) and users (numerical phantoms). The DL contribution is obtained from the assessment of the whole body SAR induced by BSs or the APs for each considered configurations. For the last, the SAR evaluation is related to the field strength at which the user is exposed. This field level can be estimated in different ways: first, through the NW to which the user is connected, second, thanks to information collected by disseminated field sensors or personal dosimeters directly worn by some users (called *exposimeters*). Information known by a NW are available at BSs or APs (individual user device transmitted (Tx) and received (Rx) powers, BS or AP Tx power and traffic load) and can be profitably used, although they don't aggregate heterogeneous data (ignoring e.g. emissions from other NWs) and are hence partial. With some software modifications or resorting to dedicated applications, Tx and Rx powers of some devices could be also known at their level, recorded and transmitted to the NW for recording and appropriate processing (notably statistical). Note that sensor and exposimeter NW can be deployed by the operators themselves or by independent external stakeholders such as regulatory agencies or local authorities. Besides these external actors, exposimeters are not only useful for a NW as they can bring complementary information about users, but also because they can provide information about their carriers who are not users or who are not currently using their devices.

This paper addresses the issue of the field level assessment and more specifically its evaluation with exposimeters. The main technical challenge resides in the modeling of the measurement errors of body-worn sensors, induced by proximity effects, notably the masking effect of the body.

A comprehensive measurement campaign was carried out with a triaxial sensor attached at three different locations on a whole body phantom. Measurements details are presented in section II and preliminary results and discussion in section III.

## II. MEASUREMENTS

Measurements were carried out with a whole body phantom in an anechoic chamber (Fig. 1a) over an ultra wide band (0.5 – 6 GHz). An EME Spy 140® dosimeter (from the company Satimo®) comprising a three-axial sensor was used to probe the far field, bypassing its internal electronics with coaxial cables directly connected to each of the three sensors. Three positions on the phantom were considered: on the "left chest", on the "left hip" and at the level of the right back pocket of trousers. This positioning was chosen based on a criterion of realistic practical use, e.g. in the internal pocket of a jacket or in a pocket of a shirt for the first, and in a front pocket of trousers or attached to the belt for the second. For each location, three distances to the body were considered (about 0, 10 and 20 mm) in order to extend the practical relevance and test the spacing influence. For each configuration and axis, the antenna transfer function $\mathcal{H}(f,\theta,\varphi)$ [1], was measured over the azimuthal plane for three elevations

(0, 20° and –16°) and two orthogonal polarizations (vertical, parallel to the rotation axis in azimuth, i.e. to the phantom, and horizontal). The reflection coefficients $S_{11}$ were also measured for each configuration. This constitutes a total measurement set of 11 691 frequency responses (comprising 162 conical cuts). All relevant quantities (realized gain $G_r$, power gain $G$ and (loaded) antenna factor $AF$) can be computed from the measured quantities, for each polarization. Each component of the field, or its magnitude, can be computed as well for a given incident power density.

## III. PRELIMINARY RESULTS

### A. Raw measurement results

An example of "raw" measurements is given in Fig. 1b showing the total Mean Realized Gain (MRG averaged over 0.7 – 6 GHz) –including all axes– in horizontal polarization. As expected, the body masking is the dominant effect, with Front to Back Ratios (FTBR) of about 13 dB (resp. 15 dB) for the Chest (resp. for the Back). The Hip case is less "unidirectional", but the MRG is globally lower, both aspect being probably due to the effect of the hand. Such high FTBRs induce a high uncertainty of the exposimeter measurements, if it is used as is, without correction strategy. In addition, because of reflections or absorption and shadowing of the body, the exposimeter gain, hence the measured field, can be either higher or significantly lower than in the absence of the carrier.

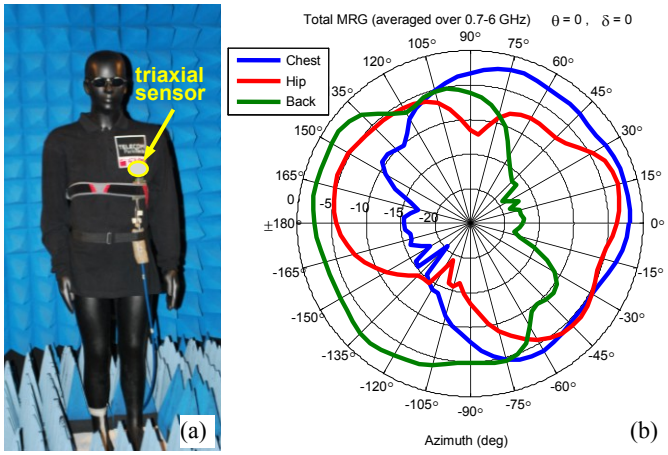


Fig. 1. (a) Measurement on a phantom in anechoic chamber (sensor on the chest), (b) Total MRG (averaged over 0.7 – 6 GHz) in the azimuthal plane (θ = 90°) measured in horizontal polarization, for a body/sensor spacing of δ = 0.

### B. Polarimetric results

#### 1) Isotropy

Although used in reception by essence, the sensor can be first characterized in emission. Indeed, the received signal at each probe port $n$ can be written as [1]:

$$b_n(f,\hat{\mathbf{r}}) = e^{-j\mathbf{k}_i\cdot\mathbf{r}}\sqrt{\frac{4\pi}{\eta_0}}\mathcal{H}_n^R(f,\hat{\mathbf{r}})\cdot\mathbf{E}_i(\mathbf{k}_i,\mathbf{r})$$

$$= -\frac{1}{2}j\sqrt{\frac{4\pi}{\eta_0}}\frac{c}{\omega}\mathcal{H}_n^T(f,\hat{\mathbf{r}})\cdot\mathbf{E}_{i0}$$

Where $\mathcal{H}^R$ (resp. $\mathcal{H}^T$) are the antenna transfer functions in the receiving (resp. transmitting) modes, $\eta_0$ thee free space impedance, $\omega$ the angular frequency, $\mathbf{k}_i$ the wave vector of the incident plane wave $\mathbf{E}_i$ and $\mathbf{E}_{i0} = \mathbf{E}_i(f,0)$ denotes the field at the origin chosen at the center of the sensor spherical ground. Apart from a frequency scaling, the directional and polarization characteristics are the same in both modes.

These characteristics are presented for both isolated and worn sensor, for the main communication bands (GSM900, GSM1800, UMTS, LTE800 & 2600, and WiFi 2.45 GHz 5.5 GHz) ; the results are averaged over each frequency band.

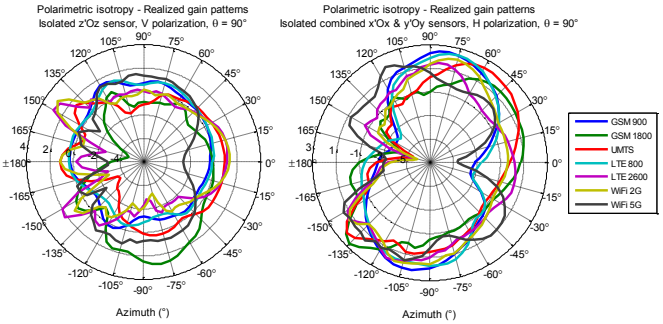


Fig. 2. Realized gain patterns in azimuth (isolated sensor), θ = 90°.

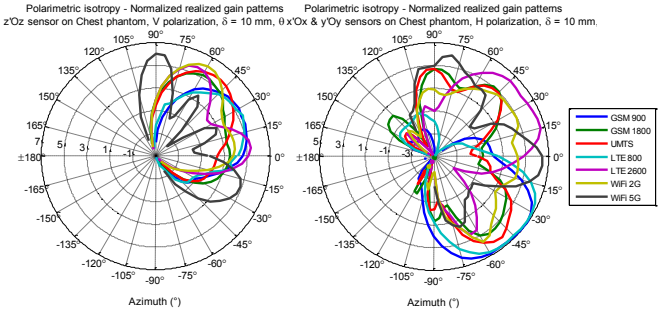


Fig. 3. Realized gain patterns in azimuth (sensor on phantom chest), θ = 90°.

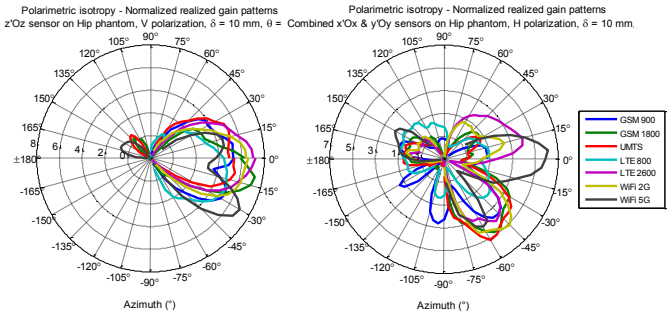


Fig. 4. Realized gain patterns in azimuth (sensor on phantom hip), θ = 90°.

We can draw a picture from these preliminary results:

- The isolated sensor "isotropy" is not perfect although its variance remains low (typ. $\sigma_G < 2$ dB),
- The variance is generally lower for the horizontal probes,
- As expected, the body proximity increases significantly the variance, i.e. the non "isotropy", particularly for the "vertical" probe (by typ. 6 to 10

dB), but less for the "horizontal" one (by 3 to 6 dB), depending on the frequency band

- The effect of the distance to the body is marginal,
- The elevation influence is moderate (Fig. 7), at least for angles close to the horizon (here less than by ± 20° around θ = 90°).

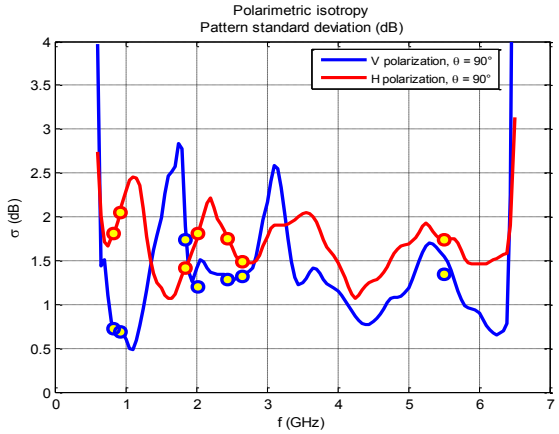


Fig. 5. Standard deviation of the realized gain patterns over azimuth (isolated sensor), θ = 90°.

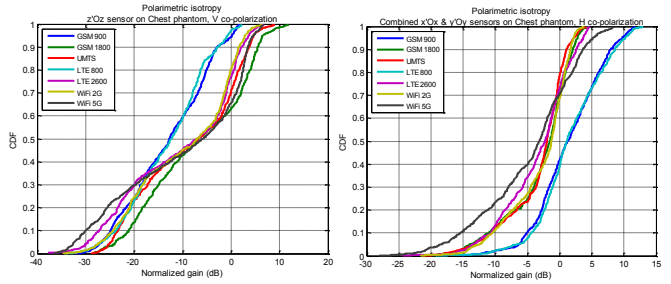


Fig. 6. Dispersion of the realized gain patterns over azimuth (sensor on chest, and hip), all δ and θ.

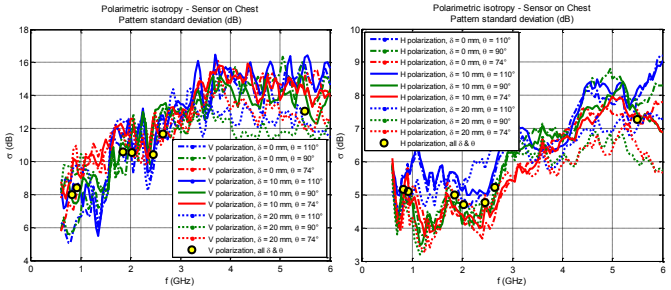


Fig. 7. Dispersion of the realized gain patterns over azimuth (sensor on chest, and hip), all δ and θ.

*2) Polarization characteristics*

The sensor probes are not purely linearly polarized, including in the isolated case (Fig. 8). This imperfection is characterized here by the cross-polarization ratio $XPR = G_r^{(cx)} / G_r^{(co)}$. For most of the cases, it is typically less than – 10 dB for the vertical probe and less than –4 dB for the higher bands (LTE & WiFi) for the horizontal probes. However the XPR is high for the upper bands of the later (up to +3 dB for the GSM900 and LTE800).

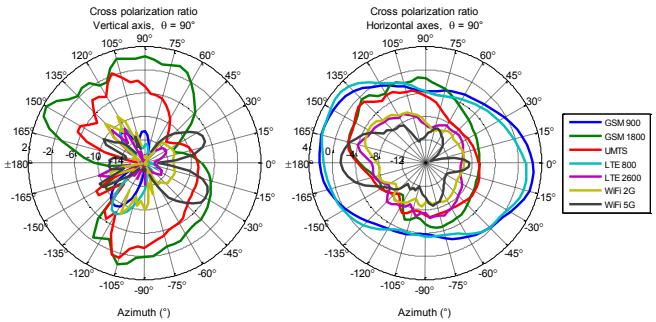


Fig. 8. XPR level (the isolated case).

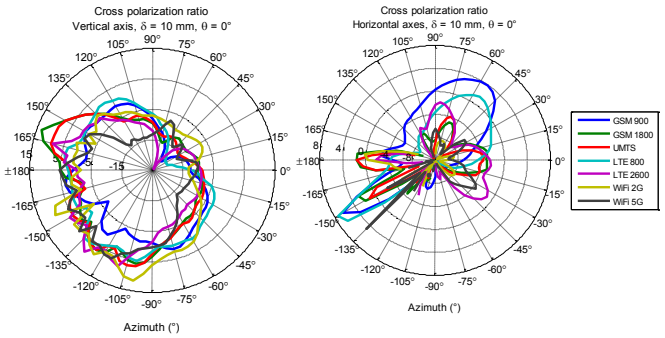


Fig. 9. XPR level (on phantom chest).

For sensor on the chest, the XPR is typically increase by 20 dB (compared to the isolated case) for the vertical probe, and up 35 dB for some directions and bands (Fig. 9). This depolarization effect due to the presence of the body is less pronounced for the horizontal sensors. Results are comparable for the Hip case. However, these high values occur in the shadow region (masked by the body). In the visible region, the XPR increase is less significant, ranging between –15 dB to 15 dB for the vertical probe horizontal and typically less than 8 dB for the horizontal ones.

*C. Polarization effects – non polarimetric approach*

Several combined polarization aspects have to be taken into account:

- First, the cross-polarization levels of the orthogonal sensors is not necessarily high, in particular for small UWB sensors, as it is the case here,
- Second the body proximity tends to increase the cross-polarization components,
- Thirds, the depolarization effect of the propagation channel is often significant: for most classical scenarios (such as those considered e.g. in the WINNER+ models), mean "V to H" cross-polarization ratios (XPR) at the terminal (UT) are typically observed in the range ~3 – 12 dB, with spreads in the range ~3 – 6 dB, depending on the considered scenario (e.g. Indoor, Outdoor to Indoor (O2I), Urban Macrocells (UMa), LOS or NLOS, etc.).

It means in particular that the sensor must be characterized in the receiving mode, taking into account the depolarization effect of the channel, i.e., as a first approach, considering different values of the incoming wave XPR. More realistically, channels models should be considered to

correctly asses the non isotropy of the sensor due the body proximity (Fig. 2 & 3).

A non polarimetric approach is considered now, i.e. that a linear combination of the power of the signal probes is evaluated: $b(f,\theta,\varphi)=\left[\frac{1}{2}(|b_1|^2+|b_2|^2)+|b_3|^2\right]^{1/2}$, where index "3" refers to the vertical probe. This combination improves in particular the sensor isotropy. In addition, this approach is justified by the significant increase of the cross-polarization levels, due to the body proximity.

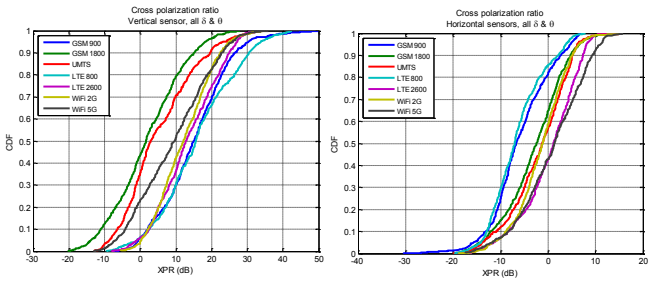


Fig. 10. Variability of the probes cross-polarization level (relative to the isolated case). The "visible region" correspond to the value around the median, typically between 30 and 60 %.

The signal *b* is computed varying the XPR ("V" to "H") of the incoming wave, from – 20 dB ("V" polarization) to + 20 dB ("H" polarization). Note that this analysis is restricted to linear polarizations. As can be observed Fig. 11 & 12, the signal variance (over the incoming wave Angle of Arrival – AoA) depends on the wave XPR. It is particularly significant for the worn sensor (Fig. 12), notably for the vertical polarization (XPR –20 dB).

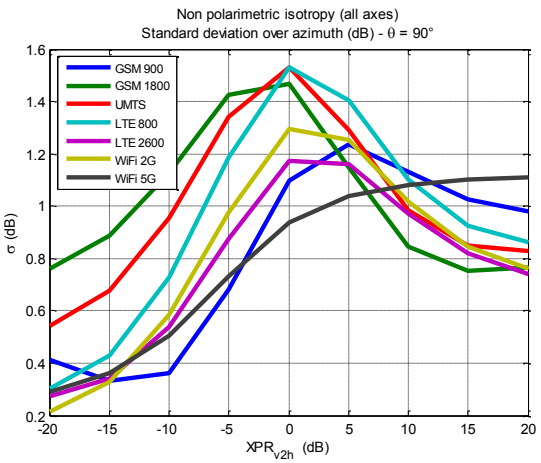


Fig. 11. Non polarimetric isotropy (isolated sensor). Variance of the received signal (over azimuth) for different incoming wave polariation.

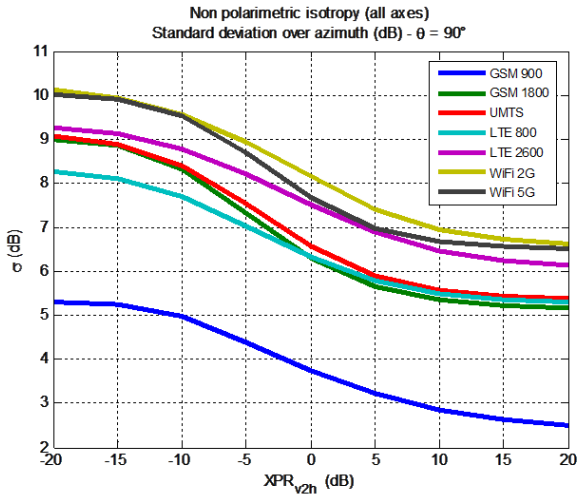


Fig. 12. Non polarimetric isotropy (sensor on Phantom's chest). Variance of the received signal (over azimuth) for different incoming wave polariation.

### *D. Possible correction Strategies*

Recently, it has been proposed in [2] to resort to several exposimeters (in this case at 950 MHz) to compensate for the shadowing and reflection effects, and somehow "regain" omnidirectionality. The results improvement of this interesting approach is really significant. However, although the system uses textile antennas and wearable electronics, one wonder if it can be easily used on a large scale, in particular with regard to its user acceptability, or if it will be restricted to professionals.

Cumulative Distribution Functions (CDF) of the MRG (proportional to the total received power) for the considered scenarios are presented in Fig. 2. As expected, the high variance observed when using only one sensor (notably in V polarization) can be drastically reduced when using two (in particular on opposite sides of the body). Using all three does not bring any improvement (note however that, contrary to the strategy adopted in [2], no attempt was made here to optimize the sensors positioning). Various other approaches [3], [4] have been proposed in the literature, in particular based on daily activity recording. Data fusion, resorting notably to GPS, accelerometers, gyrometers and magnetometers are promising.

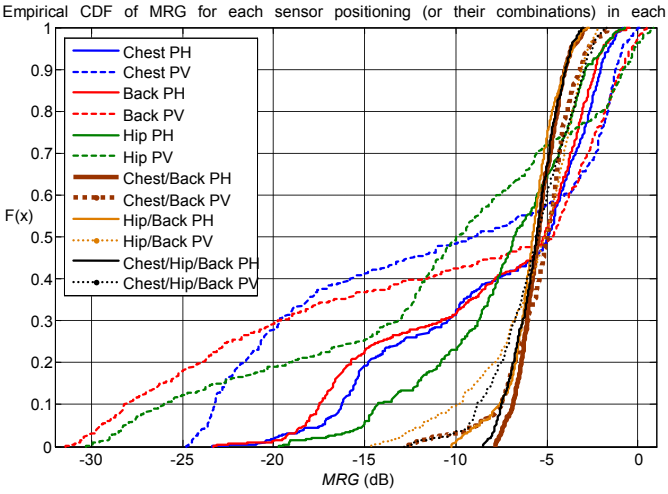

Fig. 13. Emprical CDF of the MRG for each sensor position and both polarizations, and results combining two or all positions.

## IV. CONCLUSIONS

The presented results confirm that the dispersion of measurements collected by exposimeters is large. Corrections schemes are required and will be more thoroughly discussed in the full paper. To complete these measurements data, a comprehensive simulation campaign is on-going in the framework of the Lexnet project. Its objective is to take into account other significant parameters such as anthropometric characteristics (size, corpulence, or BMI), as it is expected that their impact on shadowing effects would be significant.

## ACKNOWLEDGMENT

Authors would like to thank Orange Labs for the phantom lending, SATIMO for the dosimeter lending and its adaptation for RF transmission measurements and Antoine Khy for his contribution to the measurements. This paper reports work undertaken in the context of the project LEXNET. LEXNET is a project supported by the European Commission in the 7th Framework Programme (GA n°318273). For further information, please visit www.lexnet-project.eu.

## REFERENCES

[1] C. Roblin, S. Bories, and A. Sibille, "Characterization tools of antennas in the Time Domain," IWUWBS, Oulu, June 2003.

[2] A. Thielens *et al*, "Design and Calibration of a Personal, Distributed Exposimeter for Radio Frequency Electromagnetic Field Assessment," COST IC1004, TD(13)08033, Ghent, Belgium, 25-27 Sept. 2013.

[3] J. Blas *et al*, "Potential exposure assessment errors associated with body-worn RF dosimeters," Bio Electro Magnetics, 28(7), 2007.

[4] S. Iskra *et al*, "Factors influencing uncertainty in measurement of electric fields close to the body in personal RF dosimetry," Radiation Protection Dosimetry, 140(1), 2010.